HHS Public Access

Author manuscript

Dev Biol. Author manuscript; available in PMC 2018 January 15.

Published in final edited form as:

Dev Biol. 2017 January 15; 421(2): 204–218. doi:10.1016/j.ydbio.2016.11.017.

Defective lymphatic valve development and chylothorax in mice with a lymphatic-specific deletion of Connexin43

Stephanie J. Munger[1], **Michael J. Davis**[2], and **Alexander M. Simon**[1,*]

[1]Department of Physiology, University of Arizona, Tucson, AZ 85724, USA

[2]Dept. of Medical Pharmacology & Physiology, University of Missouri School of Medicine, Columbia, MO

Abstract

Lymphatic valves (LVs) are cusped luminal structures that permit the movement of lymph in only one direction and are therefore critical for proper lymphatic vessel function. Congenital valve aplasia or agenesis can, in some cases, be a direct cause of lymphatic disease. Knowledge about the molecular mechanisms operating during the development and maintenance of LVs may thus aid in the establishment of novel therapeutic approaches to treat lymphatic disorders. In this study, we examined the role of Connexin43 (Cx43), a gap junction protein expressed in lymphatic endothelial cells (LECs), during valve development. Mouse embryos with a null mutation in Cx43 (*Gja1*) were previously shown to completely lack mesenteric LVs at embryonic day 18. However, interpreting the phenotype of $Cx43^{-/-}$ mice was complicated by the fact that global deletion of Cx43 causes perinatal death due to heart defects during embryogenesis. We have now generated a mouse model $(Cx43^{\Delta LEC})$ with a lymphatic-specific ablation of Cx43 and show that the absence of Cx43 in LECs causes a delay (rather than a complete block) in LV initiation, an increase in immature valves with incomplete leaflet elongation, a reduction in the total number of valves, and altered lymphatic capillary patterning. The physiological consequences of these lymphatic changes were leaky valves, insufficient lymph transport and reflux, and a high incidence of lethal chylothorax. These results demonstrate that the expression of Cx43 is specifically required in LECs for normal development of LVs.

Keywords

connexin; Connexin43; gap junction; lymphatic valve; valve development; chylothorax

Introduction

The lymphatic system encompasses an ordered network of absorptive and conducting vessels that are essential for maintaining tissue fluid balance, immune function, and the

*Author for correspondence: Alexander M. Simon, Ph.D. Department of Physiology, University of Arizona, PO Box 245051, Tucson, AZ 85724, USA. Phone: 520-977-5818; Fax: 520-626-2382.

absorption and transport of dietary fat. Defects in the development and function of lymphatic vessels can lead to a number of congenital and acquired pathological conditions, including lymphedema, chylothorax, metabolic disorders, inflammation, and immune dysfunction (Aspelund et al., 2016; Betterman and Harvey, 2016). Critical to vessel function are the lymphatic valves (LVs), cusped luminal structures which ensure that lymph moves in the forward direction only, propelled in part by intrinsic contractions of the lymphatic vascular smooth muscle cells (Bazigou and Mäkinen, 2012). In some instances, congenital valve aplasia or agenesis may be a direct cause of lymphatic disease, as is likely the case with lymphedema-distichiasis syndrome (Kriederman et al., 2003; Petrova et al., 2004) and Emberger syndrome (Kazenwadel et al., 2015a; Sweet et al., 2015). A number of proteins responsible for coordinating LV formation have been identified in recent years, including gene-specific transcription factors, some regulated by disturbed fluid flow, as well as several cell surface receptors and their ligands (Yang and Oliver, 2014; Kazenwadel et al., 2016; Aspelund et al., 2016). Understanding the molecular mechanisms operating during LV development and maintenance will be an important step in establishing novel therapeutic approaches to treat lymphatic disorders.

Connexins (Cxs) are a family of proteins recently shown to be critical for LV formation, but their role during valve development is not well understood. Members of this family (21 members in humans) typically form gap junction intercellular channels, allowing for the direct cell-to-cell transfer of small molecules, including second messengers, but Cxs can also assemble into undocked hemichannels that open transiently to release extracellular signals (Goodenough and Paul, 2009; Evans, 2015). In addition, Cxs may contribute to signaling that is independent from their channel function, by functionally interacting with other vital cellular proteins (Laird, 2010; Zhou and Jiang, 2014; Leo-Macias et al, 2016).

Three Cx family members (Cx37, Cx43, and Cx47) are expressed in murine lymphatic endothelial cells (LECs) and become enriched at LVs, where they are differentially expressed on the upstream and downstream faces of the valve leaflets (Kanady et al., 2011; Kanady and Simon, 2011). Deletion or mutation of these Cx genes results in lymphatic defects in both mice and humans. *CX47* gene (*GJC2*) mutations, for example, have been identified in some families exhibiting dominantly inherited lymphedema (Ferrell et al., 2010). In addition, late-onset lymphedema segregated with affected members in a family with oculodentodigital syndrome, a disorder caused by a mutation in the *CX43* gene (*GJA1*) (Brice et al., 2013). In mice, a null mutation in *Cx37* resulted in defective LV development as well as a complete absence of venous valve formation (Kanady et al., 2011; Sabine et al., 2012; Munger et al., 2012). Furthermore, when a Cx37 null mutation was combined with the loss of a single copy of *Cx43*, the outcome was adult $Cx37^{-/-}Cx43^{+/-}$ mice with substantial lymphatic reflux and a high incidence of sudden lethal chylothorax. In an even more severe model, $Cx37^{-/-}Cx43^{-/-}$ embryos, lacking both Cxs entirely, exhibited bloody lymph and developed profound lymphedema in utero (Kanady et al., 2011).

There is evidence that Cx43 is necessary for the formation of LVs. Mouse embryos with a null mutation in Cx43 displayed a striking phenotype characterized by the complete absence of mesenteric LVs and an abnormally patterned thoracic duct (Kanady et al., 2011). However, interpretation of the phenotype of mice with a conventional, global knockout of

Cx43 was somewhat complicated, first, by the fact that Cx43 is widely expressed during embryogenesis and, second, because *Cx43*$^{-/-}$ mice die perinatally due to developmental heart defects (Reaume et al., 1995). Thus, it was difficult to rule out the possibility that some of the lymphatic defects in *Cx43*$^{-/-}$ mice could be due to the loss of Cx43 from cell-types other than LECs or that lymphatic defects could in some way be secondary to the cardiac defects.

In this study, we have addressed these issues of specificity by generating a mouse model with a tissue-specific inactivation of the *Cx43* gene, using the Cre-lox system (Sauer and Henderson, 1988). In *Cx43*$^{\Delta LEC}$ mice, Cre expression is driven by the *Lyve-1* gene promoter to efficiently and much more specifically ablate Cx43 from LECs. We demonstrate that most *Cx43*$^{\Delta LEC}$ mice survive to adulthood, thereby circumventing the perinatal lethal heart defects found in *Cx43*$^{-/-}$ mice. However, although initially viable, *Cx43*$^{\Delta LEC}$ mice exhibit lymphatic functional deficits, including valve defects, and are prone to lethal chylothorax.

Materials and Methods

Mice

Cx43 (*Gja1*)-floxed (*Cx43*$^{fl/fl}$) mice (Liao et al., 2001) and *Lyve-1*$^{EGFP\text{-}hCre}$ mice (Pham et al., 2010) (referred to hereafter as *Lyve-1*^{Cre} mice) were obtained from The Jackson Laboratory (JAX strain numbers 008039 and 012601, respectively) and interbred to obtain *Lyve-1*^{Cre};*Cx43*$^{fl/fl}$ mice (referred to as *Cx43*$^{\Delta LEC}$ mice). Wild-type and Cx43-floxed allele PCR was based on the protocol supplied by The Jackson Laboratory. PCR to detect *Lyve-1*$^{+/+}$ and *Lyve-1*^{Cre} alleles was performed according to previously established protocols, using primers Lyve-1-SF10, Lyve-1-K1-QR, and Cre-SFnew1 (Pham et al., 2010; and Jason Cyster, personal communication). With some Cx43$^{\Delta LEC}$ breeders, we noted over time that germline deletion, monitored by PCR using primers YL49 and YL50 (Liao et al., 2001), of one or more floxed Cx43 alleles had occurred. This was not surprising given reports of Cre activity in the testis of *Lyve-1*^{Cre} mice (www.informatics.jax.org). In some experiments, both *Lyve-1*^{Cre};*Cx43*$^{fl/fl}$ mice and *Lyve-1*^{Cre};*Cx43*$^{fl/-}$ mice were used, as both genotypes resulted in efficient ablation of Cx43 from LECs. Control mice for experiments were *Lyve-1*$^{+/+}$;*Cx43*$^{fl/fl\ or\ fl/+}$ and *Lyve-1*^{Cre};*Cx43*$^{+/+\ or\ fl/+}$ littermates or wild-type mice. The University of Arizona and University of Missouri IACUC Committees approved all animal protocols.

Antibodies

Primary antibodies for immunostaining were: rabbit polyclonal antibodies to Collagen IV (ColIV) (ab19808, Abcam), Cx37 (18264) (Simon et al., 2006), Cx43 (C6219, Sigma), Cx47 (364700, Invitrogen), Laminin α5 (Lam α5) (405, a gift from Lydia Sorokin; used on whole mount samples) (Sixt et al., 2001), Prospero homeobox protein 1 (Prox1) (11-002, AngioBio), Prox1 (ab11941, Abcam), α-Smooth Muscle Cell Actin (SMA), Cy3 conjugated (C6198, Sigma); rat monoclonal antibody to Cluster of Differentiation 31 (CD31) (HM1013, Hycult Biotech), Laminin α5 (Lam α5) (4G6 A2 11, a gift from Lydia Sorokin; used on frozen sections) (Sixt et al., 2001), Lymphatic Vessel Endothelial Hyaluronan Receptor 1 (LYVE-1) (14-0443, eBioscience); goat polyclonal antibodies to Integrin α9 (Itga9),

(AF3827, R&D Systems) Vascular Endothelial Growth Factor Receptor 3 (VEGFR3) (AF743, R&D Systems); chicken polyclonal antibodies to Laminin (Lam) (ab14055, Abcam). AffiniPure minimal cross reactivity secondary antibodies (conjugated to Alexa 488, Alex 555, Alexa 647, Cy3, Cy5, or Dylight 649) and Alexa 647 Streptavidin were from Jackson Immunoresearch or Invitrogen. Cx37 antibodies (18264) were directly labeled using the Alexa Fluor 555 Protein Labeling Kit (A20174, Invitrogen).

Section immunostaining

Tissue samples were frozen unfixed in Tissue-tek OCT and sectioned at 10 μm. Sections on slides were fixed in acetone at −20 °C for 10 min, blocked in PBS containing 4% fish skin gelatin, 1% donkey serum, 0.25% Triton X-100, and incubated with primary antibodies for 1.5–3 h at room temperature or overnight at 4 °C. Sections were washed with PBS containing 0.25% Triton X-100 and then incubated with secondary antibodies for 30–40 min. When directly conjugated Alexa 555-Cx37 antibodies were used in conjunction with unlabeled Cx43 or Cx47 rabbit primary antibodies, the Cx43 or Cx47 antibodies were incubated on the sections first, followed by fluorescently labeled anti-rabbit secondary antibodies and a 5% normal rabbit serum blocking step, before the Alexa 555-Cx37 antibodies were applied. Sections were mounted either in Mowiol 40–88 (Aldrich) containing DABCO or in Prolong Gold (Life Technologies) and viewed with an Olympus BX51 microscope and Photometrics CoolSnap ES2 camera or with a Zeiss LSM 510 confocal microscope.

Whole-mount immunostaining

Mesentery was fixed in 1% PFA overnight at 4 °C, washed in PBS, permeabilized with PBS containing 0.3% Triton X-100, and then blocked overnight in PBS containing 3% donkey serum and 0.3% Triton X-100. Ear tissue was treated similarly except fixation was for 1 h at room temperature. Primary and secondary antibodies, diluted in PBS containing 0.3% Triton X-100, were sequentially applied to the tissue overnight at 4 °C. Samples were mounted on slides in Citifluor mountant (Electron Microscopy Sciences). For whole-mount Prox1 immunostaining of E18.5 thoracic duct and diaphragm muscle, the procedure was the same except Vectastain Elite ABC kit (Vector Laboratories) secondary, tertiary reagents, and DAB substrate were used.

Lymphangiography with Evans blue dye

5–12 mice per genotype were anesthetized with an intraperitoneal injection of ketamine (50 mg/kg)/xylazine (20 mg/kg) and placed on a warming pad. Evans blue dye (EBD) (1% w/v) was injected intradermally into both hindpaws and a dissecting microscope was used to trace EBD transport into the iliac lymph nodes and efferent lymphatics (Kriederman et al., 2003). Hindlimb skin and mesenteric lymphatic vessels and nodes were examined for abnormal dye reflux. The thoracic cavity was opened and transport of EBD into and along the thoracic duct was evaluated. Intercostal lymphatic vessels adjacent to the thoracic duct were checked for signs of dye reflux. EBD was also injected into the ear skin to evaluate EBD transport in ear lymphatics.

Lymphatic network characteristics

For analysis of capillary networks in the ear, low magnification images (4X objective) of whole-mount LYVE-1 staining were manually segmented and area density determined using Adobe Photoshop CS4 (N=4 for control and $Cx43^{\Delta LEC}$ samples). Skeletonization of the lymphatic network was created using the Skeletonize (2D/3D) plugin of ImageJ. The AnalyzeSkeleton plugin was used to determine length density, mean vessel diameter, and branch point density as previously described (Kanady et al., 2015). Lymphatic collecting vessel patterning was assessed in P7 mesentery using low magnification panoramic images of whole-mount VEGFR3 staining, constructed from a series of images captured with a 4X objective (N=6 mesentery whole-mounts for control and $Cx43^{\Delta LEC}$ samples). The mean diameter of the large radial collecting lymphatics was determined by dividing the area of each lymphatic vessel by its linear length, measured in Photoshop (N=28 control vessels; N=26 $Cx43^{\Delta LEC}$ vessels).

Quantification of LVs

Mesenteries (5–14 mice per genotype) from E18.5 embryos, P4 pups, or P7 pups were cut into 3–4 segments and whole-mount co-immunostained in 24-well dishes for a subset of markers which highlight LVs: Prox1, CD31, Lam α5, ColIV, Itga9, and VEGFR3. The total number of LVs per mesentery was determined by counting the valves in each segment. In some experiments, the percentage of LVs with immature (stages 1–3) and mature (stage 4) leaflet morphology was also determined (Sabine et al., 2012).

Ears (6 adult mice per genotype) were separated into dorsal and ventral halves and whole-mount co-immunostained for Lam α5, LYVE-1 (expressed in initial lymphatics and pre-collecting lymphatics), and VEGFR3. LVs were counted in eight fields, using the 10x objective, spanning each ear sample and the mean LVs/mm^2 was recorded. For three ear samples of each genotype, the total number of mature LVs in LYVE-1 negative collecting lymphatics was determined. Total valve length and leaflet cusp height of mature (stage 4) LVs were measured from images using ImagePro Plus software.

Six thoracic ducts from adult *Cx43*$^{\Delta LEC}$ mice (mean age 9 weeks), including two with ongoing chylothorax, were analyzed for LVs. Following EBD lymphangiography, the thoracic duct was removed, still attached to the aorta, from just above the diaphragm muscle to the region near the top of the heart. The sample was frozen unfixed in Tissue-tek OCT and 10 μm serial sections were collected along its length (mean thoracic duct length sectioned was 9,600 μm per sample). The total number of valves per thoracic duct segment was determined. Selected slides in the series were stained with haematoxylin and eosin (H&E) or immunostained for Prox1 to confirm the identification of the thoracic duct.

Adult valve back-leak test

Popliteal lymphatic collecting vessel segments containing a single valve were dissected from 8-week-old mice, cannulated onto micropipettes and analyzed as previously described (Davis et al., 2012; Scallan et al., 2013). Output pressure, downstream of the valve, was elevated while monitoring pressure, using a servo-nulling micropipette, on the input (upstream) side of the valve. Three replicate tests were performed per sample at low pressure

(0.5–10 cm H_2O at a ramp rate of 18 cm H_2O/min). Six *Cx43*$^{\Delta LEC}$ valves and 4 control (*Cx43*$^{fl/fl}$) valves were analyzed. With *Cx43*$^{\Delta LEC}$ popliteal lymphatics, shorter or abnormal looking valves were preferentially selected for analysis if present. However, at least one popliteal valve from each mouse was tested, even if all the valves looked normal. Thus, the population of *Cx43*$^{\Delta LEC}$ valves tested ranged in appearance from abnormally short to normal in length.

In situ imaging of vein valves

Anesthetized mice (N≥7 mice per genotype) were exsanguinated by clipping the right atrium. Brachial veins and superficial caudal epigastric veins were examined for venous valves using a dissecting microscope, as previously described (Munger et al., 2016).

Results

Lymphatic-specific ablation of Cx43

To circumvent the problem of perinatal lethality associated with Cx43 null mice and to address phenotypic specificity, we generated mice with a tissue-specific inactivation of Cx43. *Cx43*-floxed (*Cx43*$^{fl/fl}$) mice (Liao et al., 2001) were interbred with *Lyve-1*^{Cre} mice (Pham et al., 2010) to generate *Lyve-1*^{Cre};*Cx43*$^{fl/fl}$ mice (referred to hereafter as *Cx43*$^{\Delta LEC}$ mice) (Fig. S1A, B). *Lyve-1*^{Cre} mice have the Cre recombinase coding sequence inserted into the *Lyve-1* locus such that Cre expression is driven by the endogenous *Lyve-1* promoter (Pham et al., 2010). LYVE-1 protein is robustly expressed by LECs during normal mouse development, including in the jugular lymph sacs at E12.5, and is also detected at some level in lymph nodes, liver sinusoids, spleen sinuses, blood vessels, endocardium and a subpopulation of macrophages (Banerji et al., 1999; Baluk and McDonald, 2008; Gordon et al., 2008). The *Lyve-1*^{Cre} mouse line has been used by others to successfully inactivate, in a lymphatic-targeted manner, the genes encoding sphingosine kinase, VEGFR2, and the chromatin remodeling enzyme CHD4 (Pham et al., 2010; Dellinger et al., 2013; Crosswhite et al., 2016). Dellinger et al. showed that *Lyve-1*^{Cre} can be used to delete floxed DNA sequences in LECs that generate collecting lymphatics and their valves, as well as lymphatic capillaries (Dellinger et al., 2013). This strategy works even though collecting lymphatics downregulate LYVE-1 because collecting vessels arise from LYVE-1 positive vessels (Mäkinen et al., 2005; Norrmén et al., 2009). Consistent with these prior studies, immunostaining of P4 or P7 mesenteric collecting lymphatics showed that LEC Cx43 was undetectable in *Cx43*$^{\Delta LEC}$ mice in contrast to the robust signal observed in control littermates (Fig. 1A–D, S1C–H). Thus, Cx43 was efficiently ablated from the LECs of *Cx43*$^{\Delta LEC}$ mice.

Cx43 expression was also eliminated in LECs specifically at LVs, as assessed in developing (P4, P7) mesenteric collecting vessel LVs (Figs. 1C, D, S1C–H) and adult thoracic duct valves (Fig. 2A, B) of *Cx43*$^{\Delta LEC}$ mice. In control valves, Cx43 was detected in LECs on the upstream face of valve leaflets (Figs. 1C, 2A), as previously reported (Kanady et al., 2011) but was absent from *Cx43*$^{\Delta LEC}$ valves (Figs. 1D, 2B). Cx37 expression, found on the downstream face of control valve leaflets (Figs. 1C, 2A), was not affected by the absence of Cx43 (Fig. 1D, 2B). Interestingly, only very low levels of Cx47 were detected in LECs of

thoracic duct valves when Cx43 was eliminated, compared to control valves (Fig. 2C–D′). In a previous study, we showed that Cx47 typically colocalizes with Cx43 in a subset of valve endothelial cells in wild-type thoracic duct (Kanady et al., 2011). Finally, the loss of Cx43 in *Cx43*$^{\Delta LEC}$ mice was highly cell-type specific, as normal Cx43 expression was observed in venous valves, arterial smooth muscle cells, cardiac myocytes, and adipose tissue (Fig. S2A–D).

Chylothorax and lymphatic dysfunction in *Cx43*$^{\Delta LEC}$ mice

Unlike mice with a conventional knockout of Cx43, *Cx43*$^{\Delta LEC}$ mice typically survived to adulthood. However, they often died suddenly of chylothorax, with a milky effusion around the heart and lungs, most likely caused by a leak or disruption of the thoracic duct or one its chyle-containing tributaries (Fig. 3A, B). In addition, abnormal accumulation of adipose tissue was observed around the heart and thoracic vertebral column in 7 out of the 14 *Cx43*$^{\Delta LEC}$ mice that exhibited chylothorax (Fig. S3). The average age at death of 14 *Cx43*$^{\Delta LEC}$ mice with chylothorax, collected over a 6 month period, was 2.3±0.5 months (all values are means±SEM; range P4 – 6 months). In total, 33 *Cx43*$^{\Delta LEC}$ mice were generated in our breeding colony during this 6 month period, so the observed frequency of chylothorax was 42%. However, this is likely an underestimate as *Cx43*$^{\Delta LEC}$ mice were often sacrificed for analysis well before 6 months of age and some of the sacrificed mice may have eventually developed chylothorax if they had been allowed to age. By comparison, chylothorax was not observed in 130 control mice during the same time period.

Chyle was observed in the intercostal lymphatics of a *Cx43*$^{\Delta LEC}$ mouse with chylothorax, an indication of chylous reflux (retrograde flow) and insufficient lymph transport (Fig. 3C, D). To further investigate whether lymph transport was deficient in *Cx43*$^{\Delta LEC}$ mice, we performed Evans blue dye (EBD) lymphangiography by injecting EBD into the dermis of the hindpaws and ear skin (Fig 3E–J). 11 out of 12 *Cx43*$^{\Delta LEC}$ mice showed abnormal EBD reflux into a network of lymphatics in the hindlimb skin associated with the injected hindpaw (Fig. 3H). All 12 of the injected *Cx43*$^{\Delta LEC}$ mice displayed EBD filling of the lumbar lymph nodes, however there was little or no filling of the thoracic duct in 10 out 12 mice (Fig. 3J). In addition, dye reflux and increased lateral dye spread was observed in 9 out of 9 ear injections (Fig. 3F). These lymphatic functional deficits were noted in *Cx43*$^{\Delta LEC}$ mice even if they were not currently exhibiting chylothorax. As controls, 5 *Cx43*$^{fl/fl}$ mice were similarly injected with EBD (Fig. 3E, G, I) and only one showed mild hindlimb skin dye reflux on one side. In all 5 *Cx43*$^{fl/fl}$ controls, lumbar lymph nodes as well as the thoracic duct filled well with EBD and, in addition, transport in ear lymphatics was normal. These results show that lymphatic vascular function was significantly impaired ($P < 0.01$, Fisher's exact test, two-tailed) in *Cx43*$^{\Delta LEC}$ mice compared with *Cx43*$^{fl/fl}$ controls.

Lymphatic vessel patterning in *Cx43*$^{\Delta LEC}$ mice

Since Cx43 is widely expressed by collecting vessel LECs during lymphatic development, we examined if the absence of LEC Cx43 affected collecting vessel patterning in *Cx43*$^{\Delta LEC}$ mice, using low magnification panoramic images of whole-mount P7 mesentery VEGFR3 immunostaining (Fig. S4). The overall hierarchical organization of lymphatic vessels in P7 *Cx43*$^{\Delta LEC}$ mesentery looked similar to controls, with collecting vessels typically following

closely the organization of the blood vessels. Collecting vessel branching was similar in *Cx43*$^{\Delta LEC}$ and control mesentery, with smaller collecting lymphatics near the intestinal wall feeding into larger diameter, radially oriented collecting lymphatics. In addition, there was no significant difference in the mean diameter of the large radial collecting lymphatics in *Cx43*$^{\Delta LEC}$ and control mesentery (83.5±4.5 μm vs. 80.0±4.4 μm, respectively). Surprisingly, however, there were changes in the patterning of lymphatic capillaries in *Cx43*$^{\Delta LEC}$ adult ear skin (Fig. S5). Although the total area density of lymphatic capillaries, detected by whole-mount LYVE-1 immunostaining, was similar in *Cx43*$^{\Delta LEC}$ and control ear (0.34±0.02 vs. 0.33±0.03), capillary length density was significantly higher in *Cx43*$^{\Delta LEC}$ ears (9.4±0.4 mm^{-1} vs. 7.4±0.3 mm^{-1}) whereas mean capillary diameter was reduced (34.3±1.6 μm vs. 45.3±2.4 μm). In addition, capillary branch point density was substantially increased in *Cx43*$^{\Delta LEC}$ ears compared to controls (73.4±4.5 branch points/mm^2 versus 45.3±1.6 branch points/mm^2).

Cx43$^{\Delta LEC}$ mice exhibit delayed LV development, reduced numbers of valves, and abnormal leaflet morphology

A previous study showed that LVs were completely absent from *Cx43*$^{-/-}$ mesentery lymphatic vessels at E18.5 (Kanady et al., 2011). To determine if valve development was similarly affected in mice with a lymphatic-specific inactivation of Cx43, we performed Prox1 and CD31 whole-mount immunostaining on E18.5 mesentery collected from *Cx43*$^{\Delta LEC}$ mice (Fig. 4B, D) and littermate controls (Fig. 4A, C). In *Cx43*$^{\Delta LEC}$ mice, the number of LEC clusters expressing high levels of the Prox1 transcription factor, indicative of developing LVs, was only 3.3% of control values (Fig. 4E). Thus, at E18.5, LV frequency was drastically reduced in *Cx43*$^{\Delta LEC}$ mice, very much reminiscent of the *Cx43*$^{-/-}$ phenotype.

Mesentery samples were also examined postnatally, at P4 and P7, to determine if LV development in Cx43$^{\Delta LEC}$ mice was permanently blocked at E18.5 or just delayed (Figs. 5, 6 and S6). Whole-mount immunostaining was done for a number of markers that highlight LVs, including Prox1, CD31, Lam α5, Itga9, Cx37 and VEGFR3, and LV frequency and maturity were evaluated. At both P4 and P7, the total number of valves per mesentery was still greatly reduced compared to controls (29.4% of control at P4; 23.6% at P7) (Fig. 5E, F). Nevertheless, there was an increase in valve number in *Cx43*$^{\Delta LEC}$ mesenteries at these postnatal stages compared with E18.5, indicating an initial delay in valve development rather than a complete block. However, at P4 and P7, the percentage of LVs that showed mature (stage 4) morphology (Sabine et al., 2012) was reduced in *Cx43*$^{\Delta LEC}$ samples compared to controls (55.8% of control at P4; 50.3% at P7) (Fig. 5E, F). Higher magnification images of immunostained LVs in P4 and P7 *Cx43*$^{\Delta LEC}$ and control mesenteries revealed that although stage 4 *Cx43*$^{\Delta LEC}$ LVs exhibited marker expression qualitatively similar to controls in most cases, many of these valves did not appear fully elongated (Fig. 6). Quantitative image analysis showed that total valve length of mature (stage 4) valves was reduced in *Cx43*$^{\Delta LEC}$ mesentery compared to controls (65.7% of control at P4; 79.6% at P7) (Fig. 7). Cusp length of the LVs was also reduced (73.3% of control at P7) (Fig. 7). Finally, the recruitment of vascular smooth muscle cells to *Cx43*$^{\Delta LEC}$ lymphatic vessels, as visualized by α-smooth muscle cell actin immunostaining, appeared normal at P7 (Fig. 6I, J).

In adult *Cx43*$^{\Delta LEC}$ mice, the number of valves in mesentery lymphatics remained low. However, despite the delayed and reduced frequency of valve development, there were nevertheless some mature LVs present in adult *Cx43*$^{\Delta LEC}$ mesentery (Fig. S7).

We also examined adult ear skin by whole-mount immunostaining for Lam α5, VEGFR3, and LYVE-1 (Fig. 8A–H, S8). As with mesentery, the number of LVs was substantially lower in *Cx43*$^{\Delta LEC}$ ear lymphatics compared to controls (26.8% of control) (Fig. 8I). Control ear samples contained two morphologically distinct types of LVs, depending on whether or not the lymphatic vessel was LYVE-1 positive (Fig. S8). The first type of valve, found in LYVE-1 positive pre-collecting lymphatics of the dermis, was crescent-shaped with short leaflets (Fig. S8A–C); these were also noted at transition points connecting the pre-collecting lymphatics to LYVE-1 negative collecting lymphatics (Fig. S8D–F). The second type of valve, found only within subcutaneous LYVE-1 negative collecting lymphatics, was more elongated or flame-shaped (Figs. 8A, C, E, G S8G). These collecting vessel valves, in particular, were greatly reduced in number in *Cx43*$^{\Delta LEC}$ ears (10.5% of control) (Fig 8B, I). In addition, we observed several examples of abnormal valve morphology in the collecting lymphatics of *Cx43*$^{\Delta LEC}$ ears, such as only one valve leaflet being present or misaligned leaflets (Fig. 8D, F and S8H).

The high incidence of chylothorax in *Cx43*$^{\Delta LEC}$ mice suggested a potential defect in thoracic duct valve development. To investigate this possibility, 6 adult *Cx43*$^{\Delta LEC}$ thoracic duct specimens (mean age 9.0 weeks), extending from diaphragm to heart, were serially sectioned in transverse orientation. Three of the *Cx43*$^{\Delta LEC}$ samples tested had no thoracic duct valves present and the other three samples had only one valve. Using the same methodology, we previously reported that wild-type adult mice of a similar age (mean age 10.6 weeks) typically had 3–4 valves in the superior half of the thoracic duct (Kanady et al., 2011). Thus, when compared to this control group (N=5), *Cx43*$^{\Delta LEC}$ thoracic ducts contained only 15.6% of the number of valves found in wild-type mice (0.50±0.22 valves/duct vs. 3.20±0.37 valves/duct; $P<0.0001$; unpaired t test, two-tailed). Besides the valve deficiency, thoracic duct morphology in adult *Cx43*$^{\Delta LEC}$ mice looked otherwise normal, except for one instance of bilateral thoracic duct. At E18.5, *Cx43*$^{\Delta LEC}$ thoracic duct gross morphology also appeared similar to controls, when visualized by whole-mount Prox1 immunostaining (Fig. S9).

Consistent with the lymphatic-specific nature of the gene deletion, venous valves, detected both by immunostaining (Fig. S2A) and by in situ imaging of intact vessels (Fig. S10), were unaffected in *Cx43*$^{\Delta LEC}$ mice.

Functional defects in LVs of adult Cx43$^{\Delta LEC}$ mice

To determine if there were functional consequences to the abnormal valve morphology in *Cx43*$^{\Delta LEC}$ mice, we performed valve back-leak tests on isolated, cannulated popliteal lymphatic vessel segments from adult mice (Fig. 9). Valves were subjected to elevations of output pressure while monitoring pressure on the input side of the valve. A graph of mean back pressure versus output pressure showed an overall decrease in resistance in *Cx43*$^{\Delta LEC}$ valves compared to control (*Cx43*$^{fl/fl}$) valves (Fig. 9B). Out of the 6 *Cx43*$^{\Delta LEC}$ valves tested, 4 showed some degree of leakiness whereas 2 others showed normal function. Leaky

Cx43$^{\Delta LEC}$ valves had shorter leaflet cusp lengths compared to control valves. None of the control valves showed evidence of leakiness (N=4). These results indicate a variable defect in valve function in a subset of LVs in adult *Cx43*$^{\Delta LEC}$ mice.

Discussion

Using a *Lyve-1*^{Cre} knock-in allele to drive Cx43 deletion in LECs avoided the perinatal lethality associated with *Cx43*$^{-/-}$ mice and allowed a more direct test of LEC Cx43 necessity for lymphatic development. The absence of LEC Cx43 caused a delay in LV initiation, an increase in immature valves with incomplete elongation of LV leaflets, a reduction in total valve number, and altered lymphatic capillary patterning. The physiological consequences were insufficient lymph transport, reflux, leaky valves, and chylothorax. Our studies focused on valve development, but further analysis is required to rule out possible additional roles of Cx43 in lymphatic vessel contractility, in the conduction of contractile waves, and in vessel integrity.

Chylothorax in *Cx43*$^{\Delta LEC}$ mice

Chylothorax in *Cx43*$^{\Delta LEC}$ mice most likely results from overburdening and rupture of the thoracic duct or intercostal lymphatics due to the deficiency in valves, including those in the thoracic duct. The chylothorax phenotype is similar to *Cx37*$^{-/-}$*Cx43*$^{+/-}$ mice which also exhibit a severe reduction in thoracic duct valves (Kanady et al., 2011). In contrast, chylothorax is extremely rare in *Cx37*$^{-/-}$ mice (1 case out of ~300 mice), which have a milder deficiency in thoracic duct valves (Kanady et al., 2011). Thus, chylothorax correlates with the severity of thoracic duct valve deficiency in these mouse models, and Cx43 may have a unique role in the formation of thoracic duct valves. An additional feature of *Cx43*$^{\Delta LEC}$ mice was abnormal adipose accumulation in the thoracic cavity. Adipose buildup has been reported in other mouse models with lymphatic vascular dysfunction, and may be caused by an adipogenic stimulus, such as free fatty acids, present in lymph that has leaked into the tissue (Harvey et al., 2005; Harvey, 2008; Escobedo et al., 2016). Dysfunctional lymph transport could also potentially contribute to the process of adipose accumulation (Escobedo et al., 2016).

Cx43 and lymphatic patterning

The altered capillary patterning in *Cx43*$^{\Delta LEC}$ ear skin, with smaller diameter vessels and increased branching, was surprising since Cx43 was not detected in the LYVE-1 positive lymphatic capillaries of the adult ear (Kanady et al., 2011). However, it remains possible that Cx43 is expressed by developing lymphatic capillary LECs during embryogenesis and is down-regulated postnatally. Alternatively, the valve deficiency in collecting vessels could have secondary effects on capillary patterning by altering upstream flow patterns.

Cxs and the early stages of valve development

Cx43$^{\Delta LEC}$ mice revealed a delay in LV formation in the absence of LEC Cx43, rather than complete valve agenesis as first suggested by *Cx43*$^{-/-}$ embryos (Kanady et al., 2011). Lymphatic-specific deletion of Cx43 allowed an examination of both embryonic and postnatal stages, whereas *Cx43*$^{-/-}$ mice die around birth due to heart defects (Reaume et al.,

1995). A limitation of the present study is that although LEC Cx43 was not detected in *Cx43*$^{\Delta LEC}$ mice at P4 or P7, it is difficult to rule out the possibility that delayed LV formation in *Cx43*$^{\Delta LEC}$ mice, rather than complete valve agenesis, is due to LEC Cx43 expression at an earlier developmental stage. However, the *Lyve-1* promoter driving Cx43 gene inactivation is widely expressed in LECs at early stages of lymphatic vessel development, before valve formation occurs. In the developing mesentery, LYVE-1 expression in the lymphatic capillaries begins around E14 and by E16 almost all of the LECs express high levels of LYVE-1 (Norrmén et al., 2009). Using the same *Lyve-1*^{Cre} allele, Crosswhite et. al showed that CHD4 is efficiently deleted from *Lyve-1*^{Cre}; Chd4$^{fl/fl}$ LECs by E14.5 (Crosswhite et al., 2016). LV formation in the mesenteric collecting lymphatics, which are derived from the LYVE-1 positive lymphatic capillaries, does not begin until E16. Thus, in *Cx43*$^{\Delta LEC}$ mice, Cx43 should be deleted in mesenteric LECs before LV development begins.

The signals that induce valve formation in lymphatic vessels are still being determined, but both extrinsic factors, such as fluid shear stress, and intrinsic genetic programs are likely involved (Sabine and Petrova, 2014; Kazenwadel et al., 2015a; Sweet et al., 2015). Previous studies showed that Cx37 plays a critical role in the early stages of valve formation (Kanady et al., 2011; Sabine et al., 2012; Geng et al., 2015). Like Cx37, Cx43 is highly expressed in LECs in embryonic lymphatic vessels (Kanady et al., 2011). However, in contrast to Cx37, which in cultured LECs is jointly regulated by oscillating shear stress and the forkhead transcription factor Foxc2, Cx43 expression is repressed by oscillating shear stress and is not dependent on Foxc2, indicating that the two family members are regulated by different signaling pathways (Sabine et al., 2012). During embryogenesis, there is widespread early expression of Cxs in the lymphatic as well as venous endothelium (Kanady et al., 2011; Munger et al., 2016). As development proceeds, Cx37 and Cx43 become highly enriched at valves but are differentially expressed on the two sides of the valve leaflet, with Cx43 present on the upstream face of the valve leaflet and Cx37 on the downstream face (Kanady et al., 2011; Munger et al., 2016).

Cx43 and valve leaflet elongation

The short LV leaflets in *Cx43*$^{\Delta LEC}$ mice indicates that Cx43 is required for full leaflet elongation. A similar role for Cx43 may occur during venous valve development (Munger et al., 2016). In cardiac neural crest cells and embryonic cortical neurons, Cx43 is required for directed cell migration, raising the possibility that Cx43 could play an analogous role during valve formation (Kameritsch et al., 2011; Matsuuchi and Naus, 2012; Kotini and Mayor, 2015). Valve leaflet formation involves the elongation, reorientation and coordinated migration of valve-forming endothelial cells (Tatin et al., 2013). Experiments with mouse embryonic fibroblasts suggest that Cx43 plays a role in directed migration by regulating the tubulin cytoskeleton and cell polarity in a channel independent fashion (Francis et al., 2011). Cx43 also interacts with the actin-binding ZO1 protein and associates with other actin-binding proteins (Toyofuku et al., 1998; Giepmans and Moolenaar, 1998; Ambrosi et al., 2016). The Sema3A/Nrp1/PlexinA1 pathway is required for normal LV elongation, and a common downstream target of this pathway is the organization of the actin cytoskeleton (Jurisic et al., 2012; Bouvrée et al., 2012). Moreover, when cardiac neural crest cells were

isolated from *Cx43*$^{-/-}$ embryos, their cell processes failed to retract normally in response to semaphorin 3A (Xu et al., 2006). Thus, one possibility is that Cx43 influences cell migration during valve development via protein-protein interactions with signaling components that affect the cytoskeleton.

Cx43$^{\Delta LEC}$ mice versus Cx43$^{-/-}$ mice

Despite similar LV deficiencies at E18.5, there were differences in the phenotype of *Cx43*$^{\Delta LEC}$ mice versus *Cx43*$^{-/-}$ mice. In *Cx43*$^{-/-}$ embryos, the thoracic duct was grossly erratic in caliber at E18.5, with blind-ended outcroppings and bifurcated segments, and the lymphatic network on the diaphragm muscle was greatly reduced (Kanady et al., 2011). These defects were not observed in *Cx43*$^{\Delta LEC}$ embryos (Fig. S5), however, suggesting either a very early requirement for Cx43 in LECs or their precursors, before the *Lyve-1* promoter is active, or that the *Cx43*$^{-/-}$ -specific defects were due to the absence of Cx43 from a non-LEC cell-type. Cx43 is known to be expressed by mesenchymal stem cells, which can affect lymphangiogenesis (Valiunas et al., 2004; Buttler et al., 2013; Maertens et al., 2014), as well as macrophages and lymphocytes (Glass et al., 2015), which have been implicated in pathological lymphangiogenesis (Betterman and Harvey, 2016). In addition, Cx43 expression in thymic regulatory T cell precursors enhances the production of Foxp3^{+} regulatory T cells (Kuczma et al. 2011), a population of cells which were recently shown to modulate lymphedema and promote lymphatic vessel function (Gousopoulos et al., 2016). During development, lymphangiogenesis in the diaphragm is regulated by macrophages, which are closely associated with the sprouting tips of lymphatic vessels (Ochsenbein et al., 2016). However, macrophages associated with lymphangiogenesis are typically LYVE-1 positive (Kim et al., 2007; Ochsenbein et al., 2016) and therefore Cx43 in those macrophages may be deleted in *Cx43*$^{\Delta LEC}$ mice, but this remains to be determined. Cx43 could also play a role in chemokine signaling during lymphatic vessel development, with this pathway being altered in *Cx43*$^{-/-}$ mice but not *Cx43*$^{\Delta LEC}$ mice. In zebrafish, chemokine signaling is necessary for thoracic duct patterning (Cha et al., 2012). The relevant LECs in zebrafish express chemokine receptors whereas the cells secreting the chemokines lie outside the developing vessel. Moreover, there is evidence for Cx43 involvement in chemokine signaling, as CXCL12 secretion by bone marrow stromal cells is mediated by Cx43 and Cx45 gap junctions (Schahnovitz et al., 2011). In radial glial cells, CXCL12 and Cx43 colocalize at glio-vascular contacts, and it has been suggested that release of CXCL12 could be regulated by the activation of undocked Cx43 hemichannels that function as release channels (Errede et al., 2014). Thus, in addition to the direct role that Cx43 plays in LECs, it may also influence lymphatic development indirectly via its function in a non-LEC cell-type.

Ear lymphatic valves

Two lymphatic plexuses are generated in the ear by postnatal remodeling, a primary plexus of LYVE-1 down-regulated collecting lymphatics in the subcutaneous layer and a secondary plexus of LYVE-1 positive initial lymphatics in the dermis (Dellinger et al., 2008). We noted two types of LVs in the adult ear: elongated, flame-shaped valves in LYVE-1 negative collecting lymphatics and short crescent-shaped valves in LYVE-1 positive pre-collectors. Intravital staining for perlecan was previously used to describe asymmetric valves in pre-

collectors in mouse ear in contrast to bicuspid valves in collecting lymphatics (Kilarski et al., 2014). However, the combination of Lam α5, VEGFR3, and LYVE-1 immunostaining used in our study is particularly effective in visualizing differences in valve morphology. In mesentery, LVs are found in LYVE-1 down-regulated lymphatics. However, valves have been previously noted in LYVE-1 positive pre-collecting ear lymphatics (Lutter et al., 2012), in the LYVE-1 positive lymphatics of the corneal limbus (Truong et al., 2011), and in new corneal lymphatic vessels formed during inflammation (Truong et al., 2011). Our results emphasize the need to consider both varieties of ear LVs when characterizing mouse models, as one valve type may be more or less affected by a genetic modification. In $Cx43^{\Delta LEC}$ mice, the absence of Cx43 in LECs more heavily affected the development of valves in the LYVE-1 negative collecting lymphatics than in the pre-collectors.

Cx mutations and lymphedema

The phenotype of $Cx43^{-/-}$ mice first suggested a role for Cx43 in lymphatic development (Kanady et al., 2011). Subsequently, a family with oculodentodigital syndrome (ODD) provided evidence that a mutation in the *CX43* (*GJA1*) gene can be an isolated cause of lymphedema in humans (Brice et al., 2013). ODD is a rare, autosomal dominant congenital condition caused by mutations in *CX43* that affect the face, eyes, teeth, and digits (Laird, 2014). It remains to be seen if other families with ODD also exhibit lymphatic dysfunction or if this is an infrequent association. The *CX43* mutation associated with lymphedema causes an amino acid change in the second extracellular loop, known to be important in docking of hemichannels. One possibility is that the ODD *CX43* mutation acts in a dominant negative fashion rather than loss of function (Brice et al., 2013). It has been suggested that mutations in the *CX47* (*GJC2*) gene identified in some families with inherited lymphedema might be dominant negative (Ferrell et al., 2010). Significantly, Cx47 colocalizes with Cx43 on the upstream side of LV leaflets (Kanady et al., 2011). A dominant negative mutation in Cx47 or Cx43 might therefore affect the other coexpressed Cx, particularly if they co-oligomerize. In this study, we noted that Cx47 levels were greatly reduced in thoracic duct valves when Cx43 was eliminated from LECs, suggesting that the expression, assembly, or targeting of Cx47 may depend on Cx43. Furthermore, a Cx47 null mutation alone does not cause LV defects or lymphedema in mice, but a deficiency in both Cx47 and Cx43 does lead to mild lymphedema in some embryos, consistent with a dominant negative model (Munger et al., 2016). Thus, our study not only demonstrates that LEC Cx43 is required for normal development of LVs, it also raises the possibility that a dominant negative Cx47 mutation associated with inherited lymphedema, if it inhibits Cx43, might disrupt lymphatic function by negatively affecting LV development and function.

Supplementary Material

Refer to Web version on PubMed Central for supplementary material.

Acknowledgments

The authors thank Lydia Sorokin for Laminin α5 antibody and Jason Cyster for the PCR protocol for Lyve-1^{Cre} mice. Sarah Lehman contributed to the H&E analysis of adult Cx43$^{\Delta LEC}$ mesentery as a rotation student. We are grateful to John Kanady for help with gross dissections of Cx43$^{\Delta LEC}$ mice during the initial stages of this project and to Min Li for assistance with breeding and genotyping mice. We would also like to thank Marlys Witte and

John Kanady for critically reading the manuscript. This work was supported by National Heart, Lung, and Blood Institute Grants R01-HL64232 and R21-HL122443 (to AMS), R01-HL120867 and R01-HL122608 (to MJD), and by a University of Arizona Sarver Heart Center grant (Anthony and Mary Zoia Award).

References

Ambrosi C, Ren C, Spagnol G, Cavin G, Cone A, Grintsevich EE, Sosinsky GE, Sorgen PL. Connexin43 Forms Supramolecular Complexes through Non-Overlapping Binding Sites for Drebrin, Tubulin, and ZO-1. PLoS One. 2016; 11:e0157073. [PubMed: 27280719]

Aspelund A, Robciuc MR, Karaman S, Mäkinen T, Alitalo K. Lymphatic system in cardiovascular medicine. Circ Res. 2016; 118:515–530. [PubMed: 26846644]

Baluk P, McDonald DM. Markers for microscopic imaging of lymphangiogenesis and angiogenesis. Ann N Y Acad Sci. 2008; 1131:1–12. [PubMed: 18519955]

Banerji S, Ni J, Wang SX, Clasper S, Su J, Tammi R, Jones M, Jackson DG. LYVE-1, a new homologue of the CD44 glycoprotein, is a lymph-specific receptor for hyaluronan. J Cell Biol. 1999; 144:789–801. [PubMed: 10037799]

Bazigou E, Mäkinen T. Flow control in our vessels: vascular valves make sure there is no way back. Cell Mol Life Sci. 2012; 70:1055–1066. [PubMed: 22922986]

Betterman KL, Harvey NL. The lymphatic vasculature: development and role in shaping immunity. Immunol Rev. 2016; 271:276–292. [PubMed: 27088921]

Bouvrée K, Brunet I, Del Toro R, Gordon E, Prahst C, Cristofaro B, Mathivet T, Xu Y, Soueid J, Fortuna V, Miura N, Aigrot MS, Maden CH, Ruhrberg C, Thomas JL, Eichmann A. Semaphorin3A, Neuropilin-1, and PlexinA1 are required for lymphatic valve formation. Circ Res. 2012; 111:437–445. [PubMed: 22723296]

Brice G, Ostergaard P, Jeffery S, Gordon K, Mortimer P, Mansour S. A novel mutation in GJA1 causing oculodentodigital syndrome and primary lymphoedema in a three generation family. Clin Genet. 2013; 84:378–381. [PubMed: 23550541]

Buttler K, Badar M, Seiffart V, Laggies S, Gross G, Wilting J, Weich HA. De novo hem- and lymphangiogenesis by endothelial progenitor and mesenchymal stem cells in immunocompetent mice. Cell Mol Life Sci. 2014; 71:1513–1527. [PubMed: 23995988]

Cha YR, Fujita M, Butler M, Isogai S, Kochhan E, Siekmann AF, Weinstein BM. Chemokine Signaling Directs Trunk Lymphatic Network Formation along the Preexisting Blood Vasculature. Dev Cell. 2012; 22:824–836. [PubMed: 22516200]

Crosswhite PL, Podsiadlowska JJ, Curtis CD, Gao S, Xia L, Srinivasan RS, Griffin CT. CHD4-regulated plasmin activation impacts lymphovenous hemostasis and hepatic vascular integrity. J Clin Invest. 2016; 126:2254–2266. [PubMed: 27140400]

Davis MJ, Scallan JP, Wolpers JH, Muthuchamy M, Gashev AA, Zawieja DC. Intrinsic increase in lymphangion muscle contractility in response to elevated afterload. Am J Physiol Heart Circ Physiol. 2012; 303:H795–H808. [PubMed: 22886407]

Dellinger M, Hunter R, Bernas M, Gale N, Yancopoulos G, Erickson R, Witte M. Defective remodeling and maturation of the lymphatic vasculature in Angiopoietin-2 deficient mice. Dev Biol. 2008; 319:309–320. [PubMed: 18514180]

Dellinger MT, Meadows SM, Wynne K, Cleaver O, Brekken RA. Vascular endothelial growth factor receptor-2 promotes the development of the lymphatic vasculature. PLoS One. 2013; 8:e74686. [PubMed: 24023956]

Errede M, Girolamo F, Rizzi M, Bertossi M, Roncali L, Virgintino D. The contribution of CXCL12-expressing radial glia cells to neuro-vascular patterning during human cerebral cortex development. Front Neurosci. 2014; 8:324. [PubMed: 25360079]

Escobedo N, Proulx ST, Karaman S, Dillard ME, Johnson N, Detmar M, Oliver G. Restoration of lymphatic function rescues obesity in Prox1-haploinsufficient mice. JCI Insight. 2016; 1:e85096. [PubMed: 26973883]

Evans WH. Cell communication across gap junctions: a historical perspective and current developments. Biochem Soc Trans. 2015; 43:450–459. [PubMed: 26009190]

Ferrell RE, Baty CJ, Kimak MA, Karlsson JM, Lawrence EC, Franke-Snyder M, Meriney SD, Feingold E, Finegold DN. GJC2 missense mutations cause human lymphedema. Am J Hum Genet. 2010; 86:943–948. [PubMed: 20537300]

Francis R, Xu X, Park H, Wei CJ, Chang S, Chatterjee B, Lo C. Connexin43 modulates cell polarity and directional cell migration by regulating microtubule dynamics. PLoS One. 2011; 6:e26379. [PubMed: 22022608]

Geng X, Cha B, Mahamud MR, Lim KC, Silasi-Mansat R, Uddin MK, Miura N, Xia L, Simon AM, Douglas Engel J, Chen H, Lupu F, Sathish Srinivasan R. Multiple mouse models of primary lymphedema exhibit distinct defects in lymphovenous valve development. Dev Biol. 2016; 409:218–233. [PubMed: 26542011]

Giepmans BN, Moolenaar WH. The gap junction protein connexin43 interacts with the second PDZ domain of the zona occludens-1 protein. Curr Biol. 1998; 8:931–934. [PubMed: 9707407]

Glass AM, Snyder EG, Taffet SM. Connexins and pannexins in the immune system and lymphatic organs. Cell Mol Life Sci. 2015; 72:2899–2910. [PubMed: 26100515]

Goodenough DA, Paul DL. Gap junctions. Cold Spring Harb Perspect Biol. 2009; 1:a002576. [PubMed: 20066080]

Gordon EJ, Gale NW, Harvey NL. Expression of the hyaluronan receptor LYVE-1 is not restricted to the lymphatic vasculature; LYVE-1 is also expressed on embryonic blood vessels. Dev Dyn. 2008; 237:1901–1909. [PubMed: 18570254]

Gousopoulos E, Proulx ST, Bachmann SB, Scholl J, Dionyssiou D, Demiri E, Halin C, Dieterich LC, Detmar M. Regulatory T cell transfer ameliorates lymphedema and promotes lymphatic vessel function. JCI Insight. 2016; 1:e89081. [PubMed: 27734032]

Harvey NL, Srinivasan RS, Dillard ME, Johnson NC, Witte MH, Boyd K, Sleeman MW, Oliver G. Lymphatic vascular defects promoted by Prox1 haploinsufficiency cause adult-onset obesity. Nat Genet. 2005; 37:1072–1081. [PubMed: 16170315]

Harvey NL. The link between lymphatic function and adipose biology. Ann N Y Acad Sci. 2008; 1131:82–88. [PubMed: 18519961]

Jurisic G, Maby-El Hajjami H, Karaman S, Ochsenbein AM, Alitalo A, Siddiqui SS, Ochoa Pereira C, Petrova TV, Detmar M. An unexpected role of Semaphorin3A/Neuropilin-1 signaling in lymphatic vessel maturation and valve formation. Circ Res. 2012; 111:426–436. [PubMed: 22723300]

Kameritsch P, Pogoda K, Pohl U. Channel-independent influence of connexin 43 on cell migration. Biochim Biophys Acta. 2011; 1818:1993–2001. [PubMed: 22155212]

Kanady JD, Munger SJ, Witte MH, Simon AM. Combining Foxc2 and Connexin37 deletions in mice leads to severe defects in lymphatic vascular growth and remodeling. Dev Biol. 2015; 405:33–46. [PubMed: 26079578]

Kanady JD, Dellinger MT, Munger SJ, Witte MH, Simon AM. Connexin37 and Connexin43 deficiencies in mice disrupt lymphatic valve development and result in lymphatic disorders including lymphedema and chylothorax. Dev Biol. 2011; 354:253–266. [PubMed: 21515254]

Kanady JD, Simon AM. Lymphatic communication: connexin junction, what's your function? Lymphology. 2011; 44:95–102. [PubMed: 22165579]

Kazenwadel J, Betterman KL, Chong CE, Stokes PH, Lee YK, Secker GA, Agalarov Y, Demir CS, Lawrence DM, Sutton DL, Tabruyn SP, Miura N, Salminen M, Petrova TV, Matthews JM, Hahn CN, Scott HS, Harvey NL. GATA2 is required for lymphatic vessel valve development and maintenance. J Clin Invest. 2015; 125:2979–2994. [PubMed: 26214525]

Kazenwadel J, Harvey NL. Morphogenesis of the lymphatic vasculature: A focus on new progenitors and cellular mechanisms important for constructing lymphatic vessels. Dev Dyn. 2016; 245:209–219. [PubMed: 26228815]

Kilarski WW, Muchowicz A, Wachowska M, Mężyk-Kopeć R, Golab J, Swartz MA, Nowak-Sliwinska P. Optimization and regeneration kinetics of lymphatic-specific photodynamic therapy in the mouse dermis. Angiogenesis. 2014; 17:347–357. [PubMed: 23892627]

Kim KE, Sung HK, Koh GY. Lymphatic development in mouse small intestine. Dev Dyn. 2007; 236:2020–2025. [PubMed: 17576138]

Kotini M, Mayor R. Connexins in migration during development and cancer. Dev Biol. 2015; 401:143–151. [PubMed: 25553982]

Kriederman BM, Myloyde TL, Witte MH, Dagenais SL, Witte CL, Rennels M, Bernas MJ, Lynch MT, Erickson RP, Caulder MS, Miura N, Jackson D, Brooks BP, Glover TW. FOXC2 haploinsufficient mice are a model for human autosomal dominant lymphedema-distichiasis syndrome. Hum Mol Genet. 2003; 12:1179–1185. [PubMed: 12719382]

Kuczma M, Lee JR, Kraj P. Connexin 43 signaling enhances the generation of Foxp3^{+} regulatory T cells. J Immunol. 2011; 187:248–257. [PubMed: 21642545]

Laird DW. The gap junction proteome and its relationship to disease. Trends Cell Biol. 2010; 20:92–101. [PubMed: 19944606]

Laird DW. Syndromic and non-syndromic disease-linked Cx43 mutations. FEBS Lett. 2014; 588:1339–1348. [PubMed: 24434540]

Leo-Macias A, Agullo-Pascual E, Delmar M. The cardiac connexome: Non-canonical functions of connexin43 and their role in cardiac arrhythmias. Semin Cell Dev Biol. 2016; 50:13–21. [PubMed: 26673388]

Liao Y, Day KH, Damon DN, Duling BR. Endothelial cell-specific knockout of connexin 43 causes hypotension and bradycardia in mice. Proc Natl Acad Sci USA. 2001; 98:9989–9994. [PubMed: 11481448]

Lutter S, Xie S, Tatin F, Mäkinen T. Smooth muscle-endothelial cell communication activates Reelin signaling and regulates lymphatic vessel formation. J Cell Biol. 2012; 197:837–849. [PubMed: 22665518]

Mäkinen T, Adams RH, Bailey J, Lu Q, Ziemiecki A, Alitalo K, Klein R, Wilkinson GA. PDZ interaction site in ephrinB2 is required for the remodeling of lymphatic vasculature. Genes Dev. 2005; 19:397–410. [PubMed: 15687262]

Maertens L, Erpicum C, Detry B, Blacher S, Lenoir B, Carnet O, Péqueux C, Cataldo D, Lecomte J, Paupert J, Noel A. Bone marrow-derived mesenchymal stem cells drive lymphangiogenesis. PLoS One. 2014; 9:e106976. [PubMed: 25222747]

Matsuuchi L, Naus CC. Gap junction proteins on the move: Connexins, the cytoskeleton and migration. Biochim Biophys Acta. 2012; 1828:94–108. [PubMed: 22613178]

Munger SJ, Geng X, Srinivasan RS, Witte MH, Paul DL, Simon AM. Segregated Foxc2, NFATc1 and Connexin expression at normal developing venous valves, and connexin-specific differences in the valve phenotypes of Cx37, Cx43, and Cx47 knockout mice. Dev Biol. 2016; 412:173–190. [PubMed: 26953188]

Munger SJ, Kanady JD, Simon AM. Absence of venous valves in mice lacking Connexin37. Dev Biol. 2012; 373:338–348. [PubMed: 23142761]

Norrmén C, Ivanov KI, Cheng J, Zangger N, Delorenzi M, Jaquet M, Miura N, Puolakkainen P, Horsley V, Hu J, Augustin HG, Ylä-Herttuala S, Alitalo K, Petrova TV. FOXC2 controls formation and maturation of lymphatic collecting vessels through cooperation with NFATc1. J Cell Biol. 2009; 185:439–457. [PubMed: 19398761]

Ochsenbein AM, Karaman S, Proulx ST, Goldmann R, Chittazhathu J, Dasargyri A, Chong C, Leroux JC, Stanley ER, Detmar M. Regulation of lymphangiogenesis in the diaphragm by macrophages and VEGFR-3 signaling. Angiogenesis. 2016; 19:513–524. [PubMed: 27464987]

Petrova TV, Karpanen T, Norrmén C, Mellor R, Tamakoshi T, Finegold D, Ferrell R, Kerjaschki D, Mortimer P, Ylä-Herttuala S, Miura N, Alitalo K. Defective valves and abnormal mural cell recruitment underlie lymphatic vascular failure in lymphedema distichiasis. Nat Med. 2004; 10:974–981. [PubMed: 15322537]

Pham TH, Baluk P, Xu Y, Grigorova I, Bankovich AJ, Pappu R, Coughlin SR, McDonald DM, Schwab SR, Cyster JG. Lymphatic endothelial cell sphingosine kinase activity is required for lymphocyte egress and lymphatic patterning. J Exp Med. 2010; 207:17–27. [PubMed: 20026661]

Reaume AG, de Sousa PA, Kulkarni S, Langille BL, Zhu D, Davies TC, Juneja SC, Kidder GM, Rossant J. Cardiac malformation in neonatal mice lacking connexin43. Science. 1995; 267:1831–1834. [PubMed: 7892609]

Sabine A, Agalarov Y, Maby-El Hajjami H, Jaquet M, Hägerling R, Pollmann C, Bebber D, Pfenniger A, Miura N, Dormond O, Calmes JM, Adams RH, Mäkinen T, Kiefer F, Kwak BR, Petrova TV. Mechanotransduction, PROX1, and FOXC2 cooperate to control connexin37 and calcineurin during lymphatic-valve formation. Dev Cell. 2012; 22:430–445. [PubMed: 22306086]

Sabine A, Petrova TV. Interplay of mechanotransduction, FOXC2, connexins, and calcineurin signaling in lymphatic valve formation. Adv Anat Embryol Cell Biol. 2014; 214:67–80. [PubMed: 24276887]

Sauer B, Henderson N. Site-specific DNA recombination in mammalian cells by the Cre recombinase of bacteriophage P1. Proc Natl Acad Sci USA. 1988; 85:5166–5170. [PubMed: 2839833]

Scallan JP, Wolpers JH, Davis MJ. Constriction of isolated collecting lymphatic vessels in response to acute increases in downstream pressure. J Physiol. 2013; 591:443–459. [PubMed: 23045335]

Schajnovitz A, Itkin T, D'Uva G, Kalinkovich A, Golan K, Ludin A, Cohen D, Shulman Z, Avigdor A, Nagler A, Kollet O, Seger R, Lapidot T. CXCL12 secretion by bone marrow stromal cells is dependent on cell contact and mediated by connexin-43 and connexin-45 gap junctions. Nat Immunol. 2011; 12:391–398. [PubMed: 21441933]

Simon AM, Chen H, Jackson CL. Cx37 and Cx43 localize to zona pellucida in mouse ovarian follicles. Cell Commun Adhes. 2006; 13:61–77. [PubMed: 16613781]

Sixt M, Hallmann R, Wendler O, Scharffetter-Kochanek K, Sorokin LM. Cell adhesion and migration properties of beta 2-integrin negative polymorphonuclear granulocytes on defined extracellular matrix molecules. Relevance for leukocyte extravasation. J Biol Chem. 2001; 276:18878–18887. [PubMed: 11278780]

Sweet DT, Jiménez JM, Chang J, Hess PR, Mericko-Ishizuka P, Fu J, Xia L, Davies PF, Kahn ML. Lymph flow regulates collecting lymphatic vessel maturation in vivo. J Clin Invest. 2015; 125:2995–3007. [PubMed: 26214523]

Tatin F, Taddei A, Weston A, Fuchs E, Devenport D, Tissir F, Mäkinen T. Planar cell polarity protein Celsr1 regulates endothelial adherens junctions and directed cell rearrangements during valve morphogenesis. Dev Cell. 2013; 26:31–44. [PubMed: 23792146]

Toyofuku T, Yabuki M, Otsu K, Kuzuya T, Hori M, Tada M. Direct association of the gap junction protein connexin-43 with ZO-1 in cardiac myocytes. J Biol Chem. 1998; 273:12725–12731. [PubMed: 9582296]

Truong T, Altiok E, Yuen D, Ecoiffier T, Chen L. Novel characterization of lymphatic valve formation during corneal inflammation. PLoS One. 2011; 6:e21918. [PubMed: 21760922]

Valiunas V, Doronin S, Valiuniene L, Potapova I, Zuckerman J, Walcott B, Robinson RB, Rosen MR, Brink PR, Cohen IS. Human mesenchymal stem cells make cardiac connexins and form functional gap junctions. J Physiol. 2004; 555:617–626. [PubMed: 14766937]

Xu X, Francis R, Wei CJ, Linask KL, Lo CW. Connexin 43-mediated modulation of polarized cell movement and the directional migration of cardiac neural crest cells. Development. 2006; 133:3629–3639. [PubMed: 16914489]

Yang Y, Oliver G. Development of the mammalian lymphatic vasculature. J Clin Invest. 2014; 124:888–897. [PubMed: 24590273]

Zhou JZ, Jiang JX. Gap junction and hemichannel-independent actions of connexins on cell and tissue functions--an update. FEBS Lett. 2014; 588:1186–1192. [PubMed: 24434539]

Highlights

- A lymphatic-specific deletion of Cx43 was made using a Lyve-1 Cre allele.
- *Cx43*$^{\Delta LEC}$ mice exhibit insufficient lymph transport, leaky valves, and chylothorax.
- *Cx43*$^{\Delta LEC}$ mice show delayed lymphatic valve initiation and reduced valve frequency.
- *Cx43*$^{\Delta LEC}$ mice display immature valves with incomplete elongation of valve leaflets.
- Cx43 is required in lymphatic endothelial cells for normal valve development.

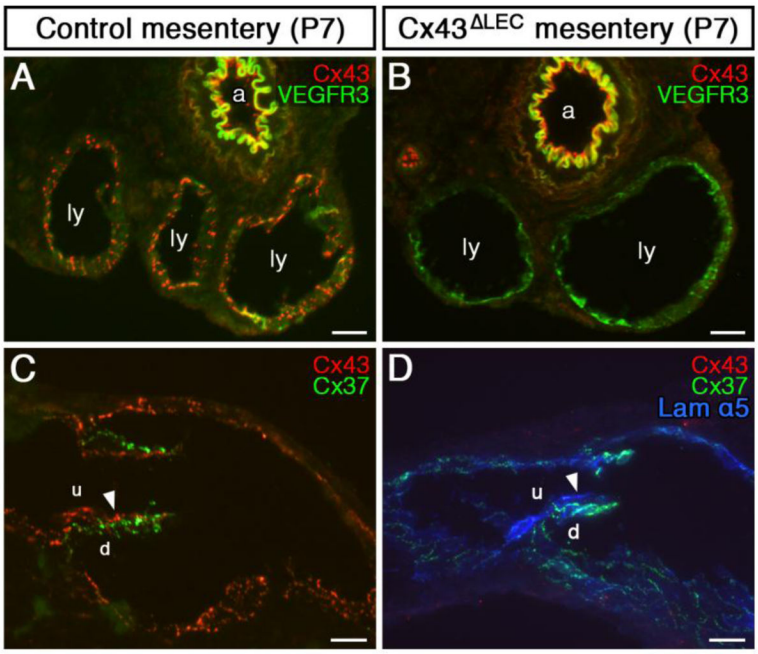

Figure 1. Cx43 is efficiently eliminated from LECs in *Cx43*$^{\Delta LEC}$ mice

Cx43 immunostaining of P7 mesentery sections showed that Cx43 was present in LECs of control *Cx43*$^{fl/fl}$ mesentery (A) and (C) but was absent from LECs of *Cx43*$^{\Delta LEC}$ mice (B) and (D). Transverse sections of lymphatic (ly) vessels are shown in (A) and (B); longitudinal sections are shown in (C) and (D). VEGFR3 staining in (A) and (B) is a marker for LECs. The intense green signal in the arteries (a) in (A) and (B) is due to autofluorescence of the internal elastic lamina. In control *Cx43*$^{fl/fl}$ LVs (C), Cx43 was detected on the upstream (u) face of valve leaflets (arrowhead), but was absent from *Cx43*$^{\Delta LEC}$ valves (D). The expression of Cx37 on the downstream (d) face of valve leaflets in control samples (C) was not affected by the absence of Cx43 in *Cx43*$^{\Delta LEC}$ valves (D). Lam α5 staining was included in (D) to highlight LV leaflets. a, artery; d, downstream; ly, lymphatic vessel; u, upstream. Scale bars: 20 μm

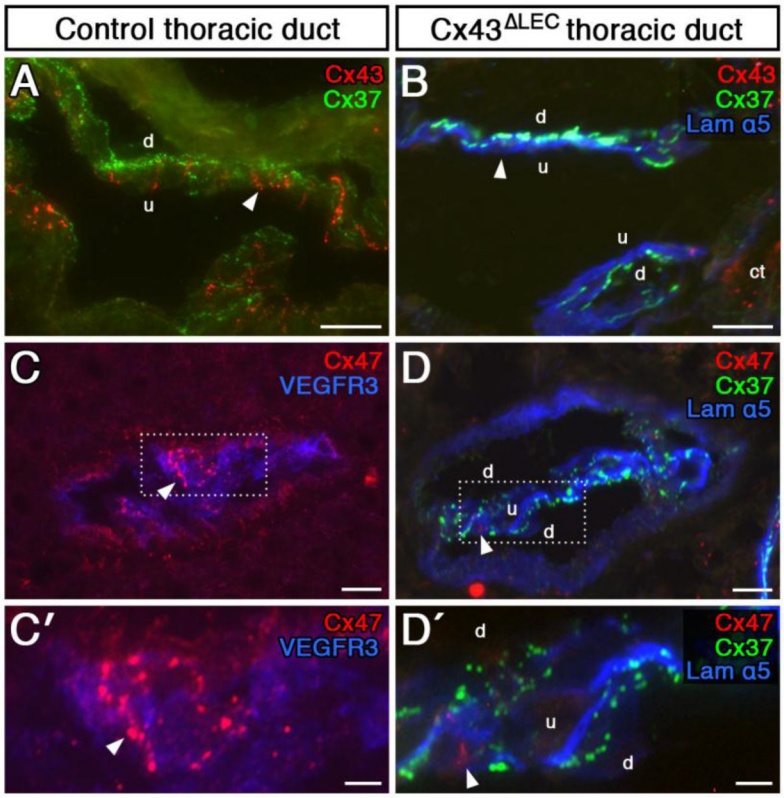

Figure 2. Deletion of Cx43 in *Cx43*$^{\Delta LEC}$ mice reduces expression of Cx47 in thoracic duct valves

Cx43, Cx37, and Cx47 immunostaining was performed on adult thoracic duct transverse sections. (A) Similar to mesenteric LVs, in control thoracic duct valves, Cx43 was detected on the upstream (u) face of valve leaflets (arrowhead) and Cx37 was found on the downstream (d) face. (B) Cx43 was absent from *Cx43*$^{\Delta LEC}$ thoracic duct valves (arrowhead), but expression of Cx37 on the downstream face of valve leaflets was unaffected by the absence of Cx43. (C) Cx47 immunostaining (arrowhead) was prominent in a subset of LECs in control thoracic duct valves, but was very low or undetectable in thoracic duct valves of *Cx43*$^{\Delta LEC}$ mice (arrowhead) (D). The boxed areas in C and D are shown at higher magnification in C′ and D′, respectively. Note that in (D) the two valve leaflets are closely apposed to each other in the section. Lam α5 staining in (B), (D), (D′) highlights the thoracic duct valve leaflets. VEGFR3 staining in (C) and (C′) is a marker for LECs. ct, connective tissue; d, downstream; u, upstream. Scale bars: 20 μm (A) – (D); 10 μm (C′) and (D′).

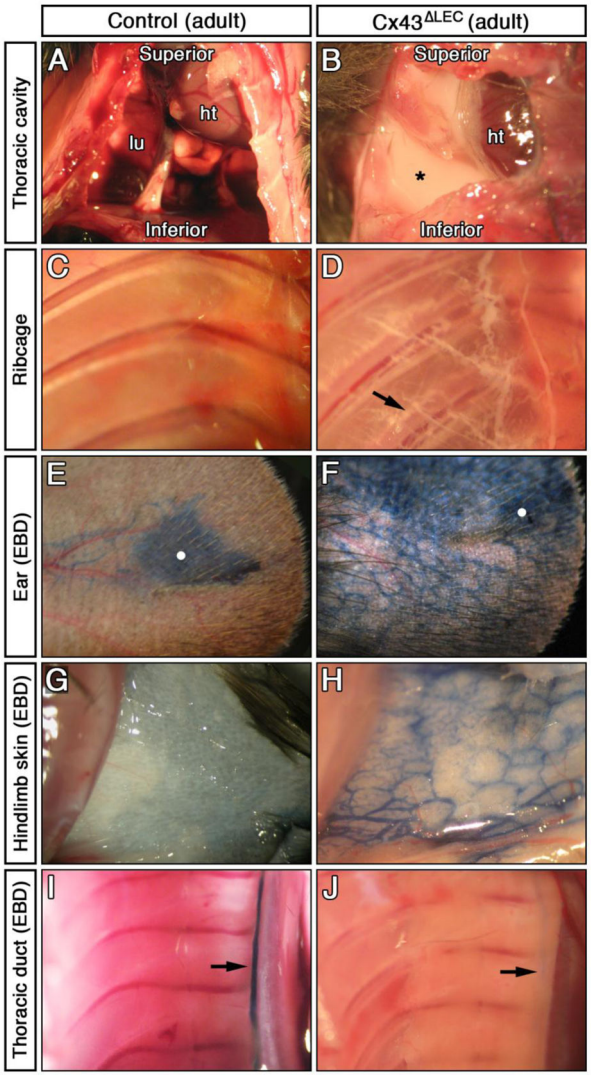

Figure 3. Chylothorax and lymphatic dysfunction in *Cx43*$^{\Delta LEC}$ mice

The chest cavity of a control mouse (A) and a *Cx43*$^{\Delta LEC}$ mouse exhibiting symptoms of chylothorax (B) was exposed. The *Cx43*$^{\Delta LEC}$ mouse showed an accumulation of chyle (asterisk) around the heart (ht) and lungs not seen in the control. Chyle was also noted in the intercostal lymphatics (arrow) of a *Cx43*$^{\Delta LEC}$ mouse with chylothorax (D), indicative of chylous reflux, but this was not observed in the control sample (C). EBD lymphangiography was performed on wild-type controls (E), (G), *Cx43*$^{flox/flox}$ controls (I), and *Cx43*$^{\Delta LEC}$ mice (F), (H), (J). Dye reflux and increased lateral spread was observed when ears of *Cx43*$^{\Delta LEC}$ mice (F) were injected with EBD, compared with ears of control mice (E). The injection site is marked by a white circle. *Cx43*$^{\Delta LEC}$ mice showed EBD reflux into a network of lymphatics in the hindlimb skin when the hindpaw was injected (H) but this reflux did not occur in control mice (G). Following hindpaw injection with EBD, there was little or no filling of the thoracic duct (arrow) in *Cx43*$^{\Delta LEC}$ mice (J) compared with control mice (I).

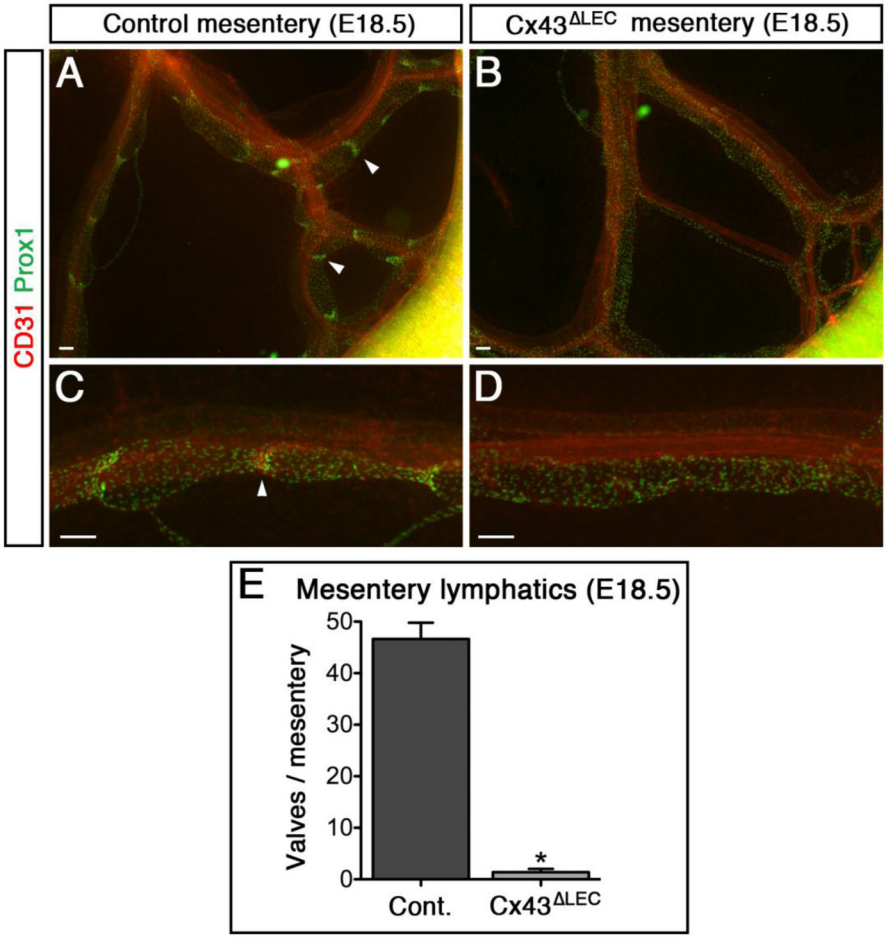

Figure 4. Mesenteric LV number is drastically reduced in *Cx43*$^{\Delta LEC}$ mice at E18.5

Prox1 and CD31 whole-mount immunostaining was performed on E18.5 mesentery collected from *Cx43*$^{\Delta LEC}$ mice (B) and (D) and littermate controls (A) and (C) to detect developing LVs. The number of LEC clusters expressing high levels of Prox1 (arrowheads), indicative of valves, was drastically lower in *Cx43*$^{\Delta LEC}$ mesenteric lymphatics compared to the controls. Lymphatics are shown at higher magnification in (C) and (D). (E) Quantification of valve counts at E18.5. Controls mesenteries (N=14) had 46.6±3.2 (mean ±s.e.m.) valves whereas Cx43$^{\Delta LEC}$ samples (N=7) had 1.57±0.81 valves (3.3% of control). *P<0.0001 versus control (unpaired t test, two-tailed). Scale bars: 100 μm.

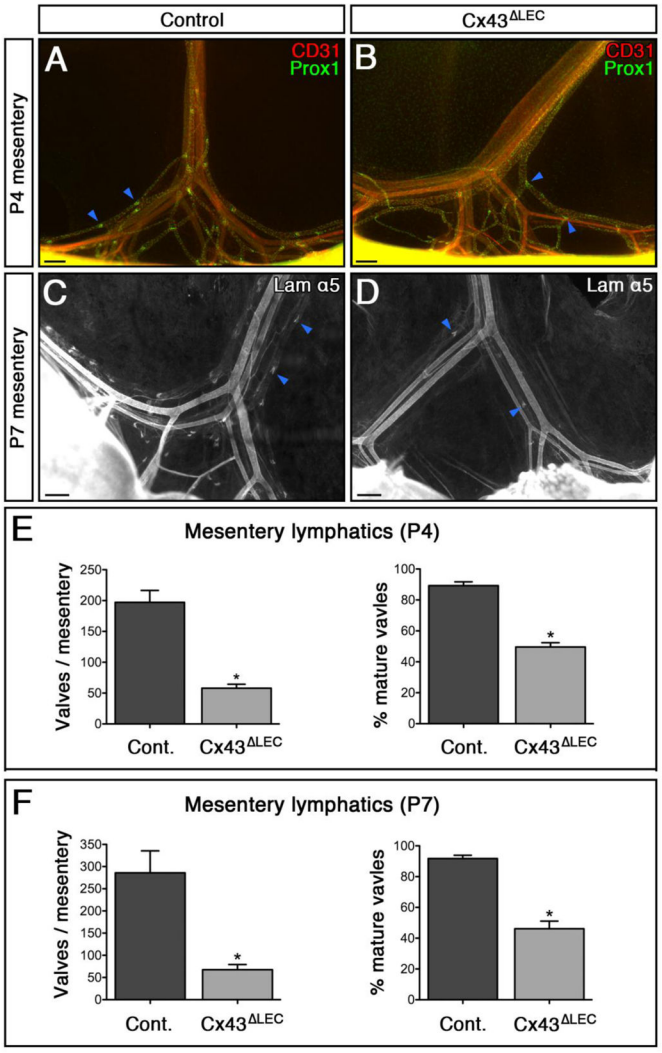

Figure 5. Mesenteric LV development is delayed in *Cx43*$^{\Delta LEC}$ mice

Prox1 and CD31 (A) and (B) or Laminin α5 (Lam α5) (C) and (D) whole-mount immunostaining was performed on P4 or P7 mesentery collected from *Cx43*$^{\Delta LEC}$ mice (B) and (D) and littermate controls (A) and (C) to detect LVs (blue arrowheads). At both P4 and P7, the total number of valves per mesentery in *Cx43*$^{\Delta LEC}$ mice was greatly reduced compared to controls (29.4% of control at P4; 23.6% at P7), however there were more valves present than at E18.5, indicating an initial delay in valve formation. The percentage of LVs that showed mature (stage 4) morphology was also reduced in *Cx43*$^{\Delta LEC}$ mesentery compared to controls. Quantification of P4 and P7 valves is presented in (E) and (F), respectively. (E) At P4, controls mesenteries (N=6) had 197.2±19.3 valves whereas *Cx43*$^{\Delta LEC}$ samples (N=7) had 58.0±6.3 valves. 88.9±1.8% of control valves were mature compared to 49.6±2.8% of *Cx43*$^{\Delta LEC}$ valves. (F) At P7, control mesenteries (N=6) contained 286.0±49.3 valves whereas *Cx43*$^{\Delta LEC}$ samples (N=5) had 67.6±11.6 valves. 91.8±2.2% of control P7 valves were mature compared to 46.2±5.0% of *Cx43*$^{\Delta LEC}$ valves. *P<0.05 versus control (unpaired t test, two-tailed). Scale bars: 200 μm.

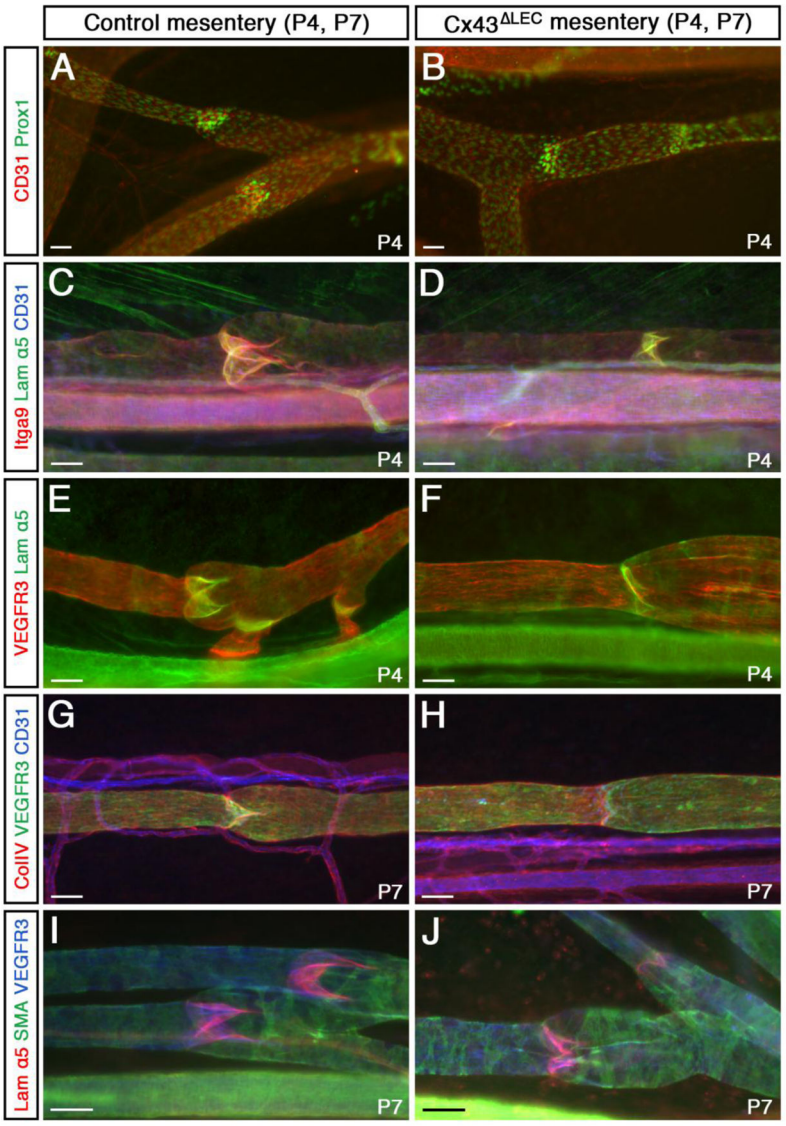

Figure 6. Mesenteric LVs in *Cx43*$^{\Delta LEC}$ mice exhibit marker expression that is similar to controls, but valve leaflets are not fully elongated

Shown are LVs from P4 or P7 *Cx43*$^{\Delta LEC}$ (B), (D), (F), (H), (J) and *Cx43*$^{fl/fl}$ control (A), (C), (E), (G), (I) mesenteries immunostained for several markers that highlight lymphatic vessels and valves. (A) and (B) Prox1; CD31. (C) and (D) Integrin α9 (Itga9); Lam α5; CD31. (E) and (F) VEGFR3; Lam α5. (G) and (H) Collagen IV (ColIV); VEGFR3; CD31. (I) and (J) Lam α5; α-Smooth Muscle Actin (α-SMA); VEGFR3. Expression of these markers appeared similar in control and *Cx43*$^{\Delta LEC}$ lymphatics, but in many cases the *Cx43*$^{\Delta LEC}$ valves did not look fully elongated. Scale bars: 50 μm.

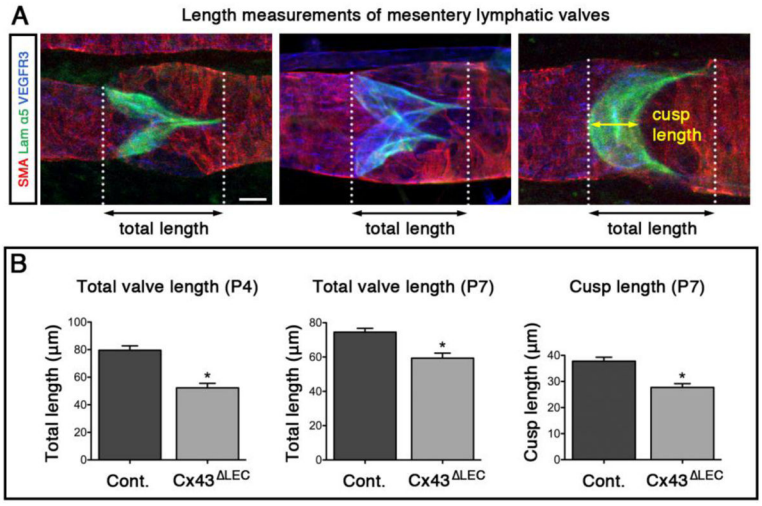

Figure 7. Total valve length and cusp length are reduced in *Cx43*$^{\Delta LEC}$ LVs

Lam α5; α-SMA; VEGFR3 whole-mount immunostaining of P4 and P7 mesenteric lymphatic vessels was used for image analysis of mature (stage 4) valves in *Cx43*$^{\Delta LEC}$ and control mice. (A) Three examples of LVs with different orientations within the vessel are shown. Dotted white lines indicate how total valve length was measured in each case. For P7 samples, cusp length was defined as the maximum length of the band of Lam α5 staining (yellow double arrow). (B) At P4, control valves (N=21) had a mean total length of 79.6±3.2 μm whereas *Cx43*$^{\Delta LEC}$ valves (N=39) were 52.3±3.3 μm (65.7% of control). At P7, control valves (N=63) had a mean total length of 74.5±2.2 μm whereas *Cx43*$^{\Delta LEC}$ valves (N=41) were 59.3±2.9 μm (79.6% of control). Cusp length in P7 *Cx43*$^{\Delta LEC}$ valves was 73.3% of controls (27.7±1.4 μm versus 37.8±1.5 μm). *P<0.0001 versus control (unpaired t test, two-tailed). Scale bars: 20 μm.

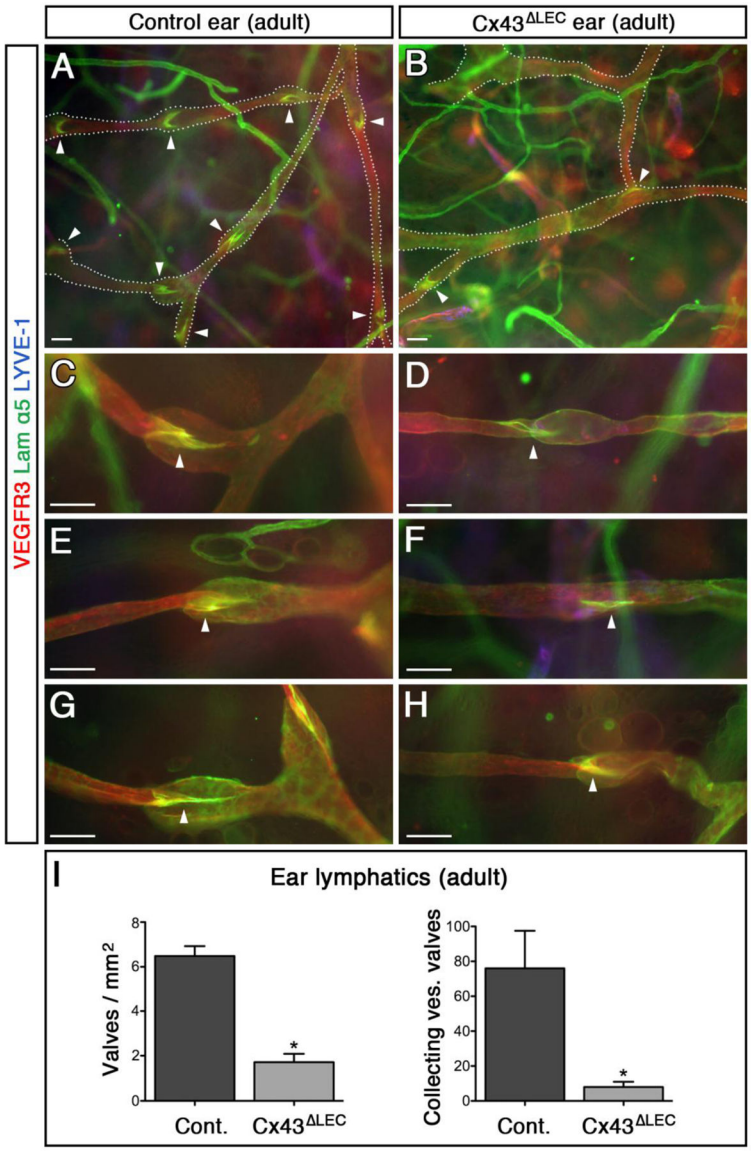

Figure 8. Reduced number and abnormal morphology of lymphatic collecting vessel valves in adult *Cx43*$^{\Delta LEC}$ ear skin

Lam α5; VEGFR3; LYVE-1 whole-mount immunostaining was performed on wild-type adult control (A), (C), (E), (G) or *Cx43*$^{\Delta LEC}$ (B), (D), (F), (H) ear skin. Two types of valves were observed in control ears: crescent-shaped valves with short leaflets in LYVE-1 positive pre-collecting lymphatics in the dermis (see Fig. S8 in the Supplemental Material section for examples of this type) and flame-shaped valves with elongated leaflets in LYVE-1 negative subcutaneous collecting lymphatics (A), (C), (E), (G). In these images, the microscope was focused on the collecting lymphatics only; LYVE-1 positive pre-collecting lymphatics are situated in a different focal plane. In (A) and (B), collecting lymphatics are outlined with white dotted lines. The total number of LVs was substantially lower in *Cx43*$^{\Delta LEC}$ ear lymphatics compared to controls (26.8% of control). Collecting vessel valves (arrowheads) in particular were severely reduced in number in *Cx43*$^{\Delta LEC}$ (A) versus control (B) ears. In

addition, abnormal valve morphology was observed in the *Cx43*$^{\Delta LEC}$ collecting lymphatics, such as only one valve leaflet being present (F) or misaligned leaflets (D). (I) Quantification of valves in *Cx43*$^{\Delta LEC}$ and control ears. Total valve density (pre-collecting and collecting vessel valves) was 6.50±0.45 valves/mm^2 (N=6) in control ears versus 1.74±0.37 valves/mm^2 (N=6) in *Cx43*$^{\Delta LEC}$ ears. Control ears had 76.0±21.5 collecting vessel valves/ear compared with only 8.0±3.0 valves/ear in *Cx43*$^{\Delta LEC}$ mice. *P<0.05 versus control (unpaired t test, two-tailed). Scale bars: 50 μm.

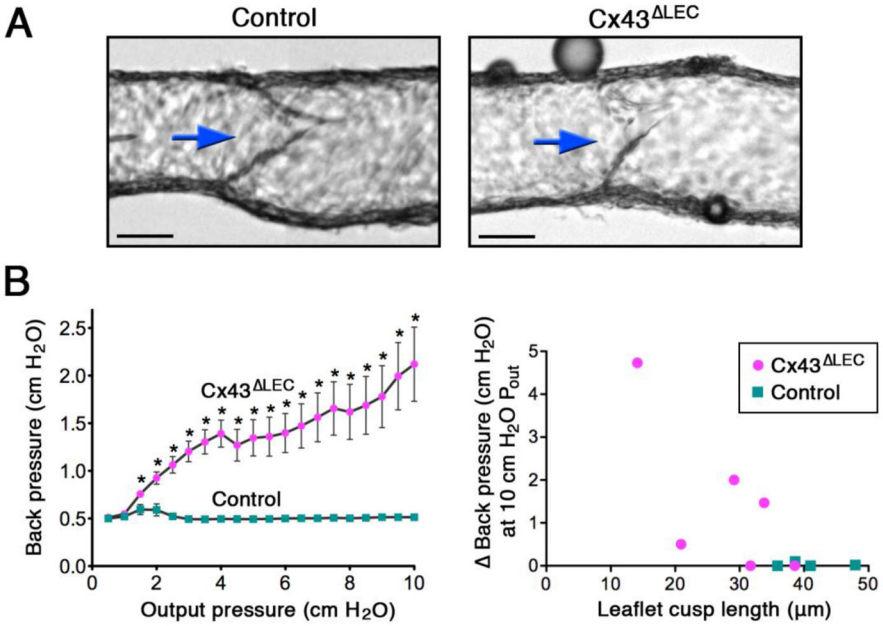

Figure 9. Functional defects in LVs of adult Cx43$^{\Delta LEC}$ mice

Valve back-leak tests were performed on isolated, cannulated popliteal lymphatic vessel segments from adult control (*Cx43$^{fl/fl}$*) and *Cx43$^{\Delta LEC}$* mice. Examples of isolated valves tested are shown in (A) with arrows indicating the normal direction of lymph flow. (B) In the graph on the left, a summary of the back-leak test data shows the overall decreased resistance of *Cx43$^{\Delta LEC}$* valves (N=6; from 5 mice) compared to control valves (N=4; from 4 mice). The graph on the right shows the change in back pressure at an output pressure (P_{out}) of 10 cm H_20 plotted versus the leaflet cusp length for each valve tested. Four out of the 6 *Cx43$^{\Delta LEC}$* valves showed varying degrees of leakiness and had shorter leaflet cusps than control valves. *P<0.05 versus control (unpaired t test, two-tailed). Scale bars: 50 μm.